Swarm Expert Support Laboratories

Swarm L2 IBI Product Description

British Geological Survey (BGS)
National Space Institute – DTU Space (DTU)
Delft Institute of Earth Observation and Space Systems (DUT)
Helmholtz Centre Potsdam - German Research Centre for Geosciences (GFZ)
Eidgenössische Technische Hochschule Zürich (ETH)
Institut de Physique du Globe de Paris (IPGP)
The Swedish Institute of Space Physics (IRF)
Laboratoire d'électronique des technologies de l'information (Leti)
University of Calgary (UoC)
Aerospace Research And Test Establishment (VZLU)

with additional contributions from

NASA Goddard Space Flight Center (GSFC)
University of Colorado (CIRES)
Charles University Prague (CUP)

Doc. no: SW-TR-GFZ-GS-0006, Rev: 2, 2017-03-18

Contents

1 Document Change Log

Issue	Issue Date	Pages Affected	Remarks	Author
1.0	27.08.2014	All	Initial Issue	J. Park
2.0	18.03.2017	5	IBI product document link is added	G. Kervalishvili

2 Applicable Documents

3 Reference Documents

RD1 Lühr, H., M. Rother, S. Maus, W. Mai, and D. Cooke (2003), The diamagnetic effect of the equatorial Appleton anomaly: Its characteristics and impact on geomagnetic field modeling, Geophys. Res. Lett., 30, 1906, doi:10.1029/2003GL017407, 17.

RD2 Stolle, C., H. Lühr, M. Rother, and G. Balasis (2006), Magnetic signatures of equatorial spread F as observed by the CHAMP satellite, J. Geophys. Res., 111, A02304, doi:10.1029/2005JA011184.

RD3 Park, J., M. Noja, C. Stolle, and H. Lühr (2013), The Ionospheric Bubble Index deduced from magnetic field and plasma observations onboard Swarm, Earth Planets Space, Vol. 65 (No. 11), pp. 1333-1344.

RD4 Swarm Level 2 Processing Facility Product specification for L2 Products and Auxiliary Products (SW-DS-DTU-GS-0001).

4 Scope

This document reports the results obtained from scientific quality validation of the Swarm Level-2 Ionospheric Bubble Index product, IBIATMS_2F, IBIBTMS_2F and IBICTMS_2F.

Current or updated version of the IBI product description document is available on the EO web page: https://earth.esa.int/web/guest/document-library/browse-document-library/-/article/swarm-level-2-ibi-product-description.

5 Introduction

5.1 Algorithm

As has been outlined by RD1, RD2, and RD3 there is an approximately linear relation between plasma density and magnetic field strength. The 1 Hz magnetic field readings of the Vector Field Magnetometer (VFM) are used for detecting plasma density irregularities. First, model values of geomagnetic field from the Earth's core, lithosphere, and magnetosphere, which are called 'mean field' in assembly, are subtracted from the VFM data. The residual field is projected onto the mean field, and the component (hereafter, 'Mean-Field-Aligned (MFA)-Z component') is high-pass-filtered (-3 dB period is approximately 24 seconds RD3) and checked for fluctuation levels. Whenever the fluctuation level of the component exceeds certain thresholds (the choice of the threshold will be discussed later), the data points are flagged by the L2-IBI processor (the contents of the flags will be shown later in Tables 1-2). The judgement based on the VFM data is further validated by the electron density data obtained from the Langmuir Probe (LP) onboard Swarm. The method is based on a cross-correlation between resampled LP data and VFM readings RD3.

5.2 Scientific Relevance

By combining electron density and magnetic field observations, L2-IBI can give information on bubble climatology itself as well as on disturbance level of magnetic field data. That is, the use of the L2-IBI product can be two-fold:

1. ionospheric scientists can easily identify equatorial plasma density irregularities.
2. magnetic field modelers can identify (and avoid) data points affected significantly by bubbles.

6 Descriptions of the data format

One data file of L2-IBI (IBIATMS_2F, IBIBTMS_2F or IBICTMS_2F) is produced per day and per satellite (Alpha, Bravo, or Charlie). However, no L2-IBI data are produced for days when either the Level 1b (L1b) electron density data (EFIA_PL_1B, EFIB_PL_1B, or EFIC_PL_1B) or magnetic field data (MAGA_LR_1B, MAGB_LR_1B or MAGC_LR_1B) are missing. The cadence of the L2-IBI data (IBIATMS_2F, IBIBTMS_2F and IBICTMS_2F) is 1 Hz, and the time stamps are synchronized with those of the corresponding L1b 1 Hz magnetic field data. The following table presents the list of variables in the L2-IBI data product. For more complete description on the input/output to the L2-IBI, readers are referred to RD4. For more complete description on the algorithm and data content, readers are referred to RD1 and RD2.

Table 1: The list of variables in the L2-IBI data product (IBIATMS_2F, IBIBTMS_2F or IBICTMS_2F).

Variable name	Description	Unit
Timestamp	Time stamps in Universal Time	cdf epoch
Latitude	Geographic latitude of the Swarm satellite	degree
Longitude	Geographic longitude of the Swarm satellite	degree
Radius	Distance of the Swarm satellite from the Earth's center	m
Bubble Index	Plasma Bubble Index	no unit
Bubble Probability	probability that the magnetic field fluctuation is related to real plasma bubbles	no unit
Flags Bubble	Flags showing the source of the magnetic field fluctuation	no unit
Flags F	Flags about the magnetic field intensity measurement (zero is nominal), passed through from the L1b data	no unit
Flags B	Flags about the magnetic field vector measurement (zero is nominal), passed through from the L1b data	no unit
Flags q	Flags about the attitude information (zero is nominal), passed through from the L1b data	no unit

Table 2: Bubble index.

Bubble Index	Description
0	Quiet data point
1	Data point affected by bubbles
-1	unanalyzable data point

Table 3: Bubble flag.

Bubble Flag	Description
0	Quiet
1	Bubble confirmed by high-correlation between plasma density and magnetic field
2	Bubble unconfirmed by high-correlation between plasma density and magnetic field
4	Large jump in magnetic field
8	Data gap
16	Pulsations in magnetic field
32	Outside the night-time low-latitude region where bubbles can be found

7 Selected Examples

Here we present three examples of L2-IBI data. Figure 1 shows a typical example of Swarm L2-IBI data. The second panel from the top shows the residual field projected onto the mean field (see Introduction), and the top panel presents residual field projected onto the mean field after high-pass-filtering and rectification. The third panel shows electron density from the Swarm/LP. We can identify strong depletions of electron density between GPS second 1073613400 and 1073614000. These depletions generate significant fluctuations in the residual field projected onto the mean field as shown in the top panel, some of which exceed the pre-defined event detection thresholds represented by horizontal dashed lines. In the bottom panel we can see that the electron density depletions are correctly identified as bubbles (Bubble Index=1, black line). Bubble Probability, which is the square of the correlation coefficient between magnetic field and plasma density, is shown as red dashed line.

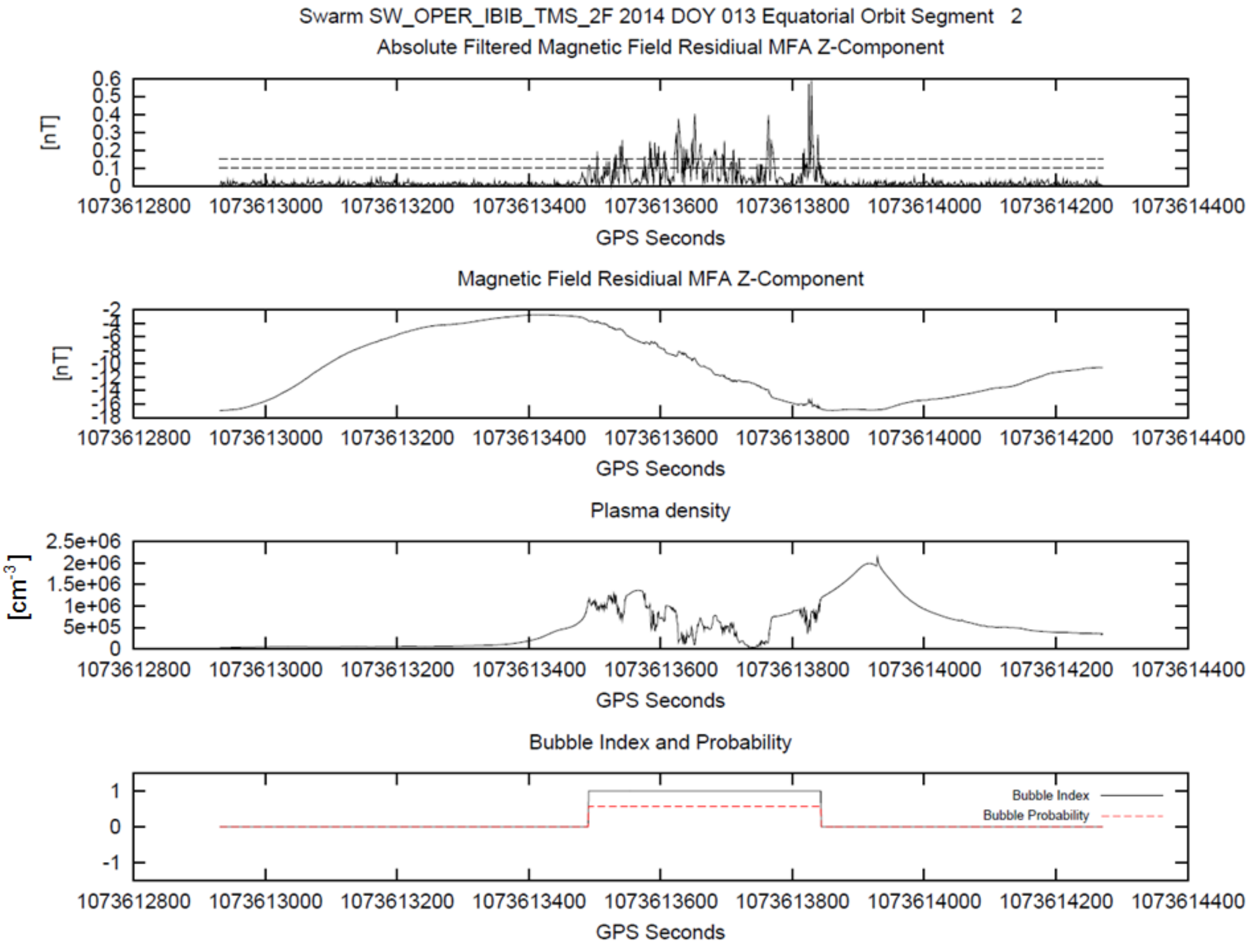

Figure 1: An example of Swarm L2-IBI data (Bubble Index=+1).

Figure 2 shows an example where the quality of VFM data is poor, and the figure format is the same as that of Figure 1. As VFM data quality is generally good in the latest versions, we should choose an example of poor quality from an older version of VFM data, which used to suffer from occasional glitches. From the top two panels we can see very strong fluctuations and jumps in the residual field projected onto the mean field (magnitude of about 35000 nT) for a large part of a satellite pass. In the bottom panel we can see that the whole pass is judged as Unanalyzable (Bubble Index=-1, black line). As a natural consequence, the corresponding Bubble Probability is zero (red dashed line).

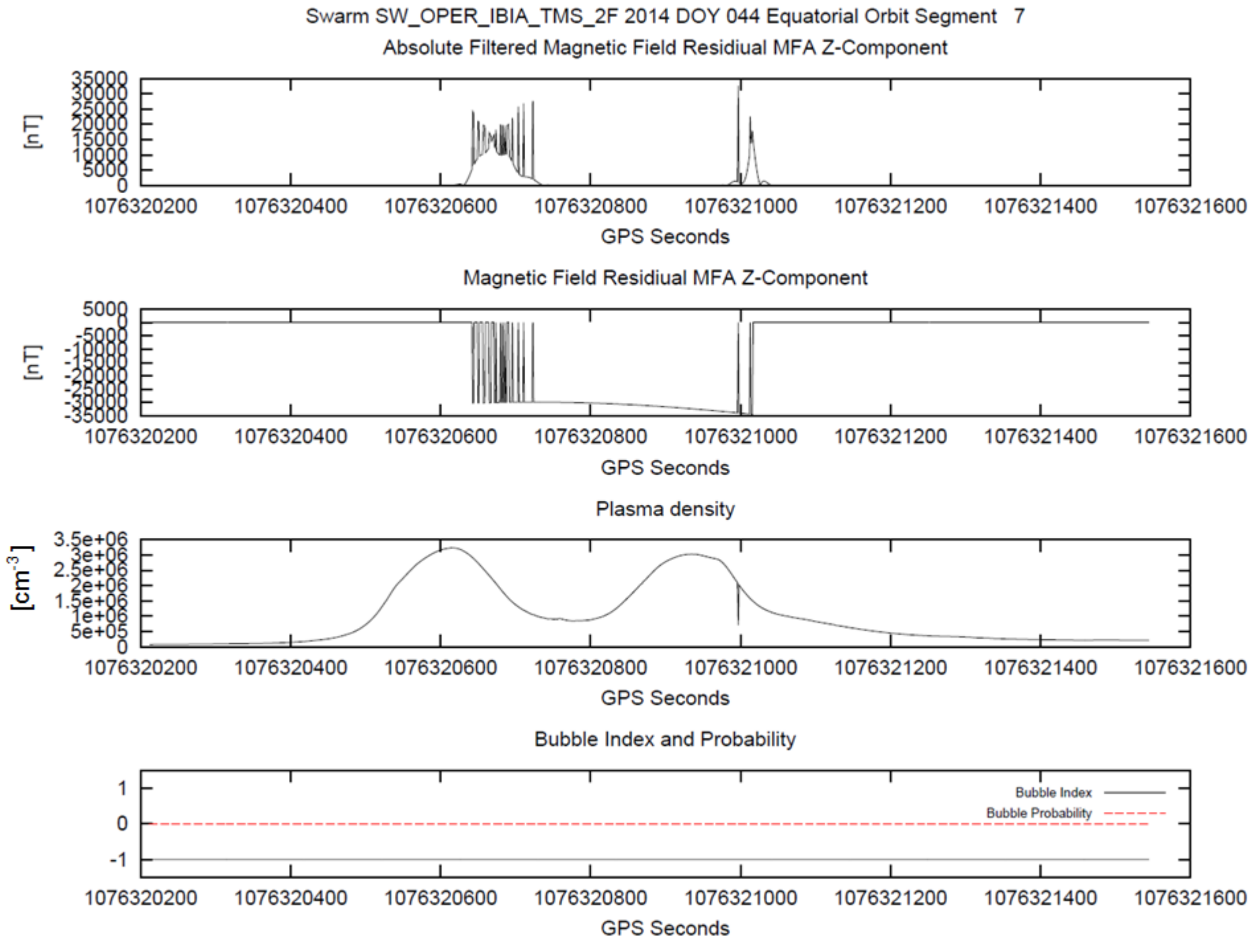

Figure 2: An example of Swarm L2-IBI data (Bubble Index=-1; Unanalyzable).

Figure 3 shows an example where the data are quiet, and the figure format is the same as that of Figure 1. From the top two panels we can see no fluctuations in the MFA z-component exceeding the threshold (dashed horizontal line). The third panel confirms that there is no irregularity in the electron density profile. In the bottom panel we can see that the whole pass is judged as Quiet (Bubble Index=0, black line). As a natural consequence, the corresponding Bubble Probability is zero (red dashed line).

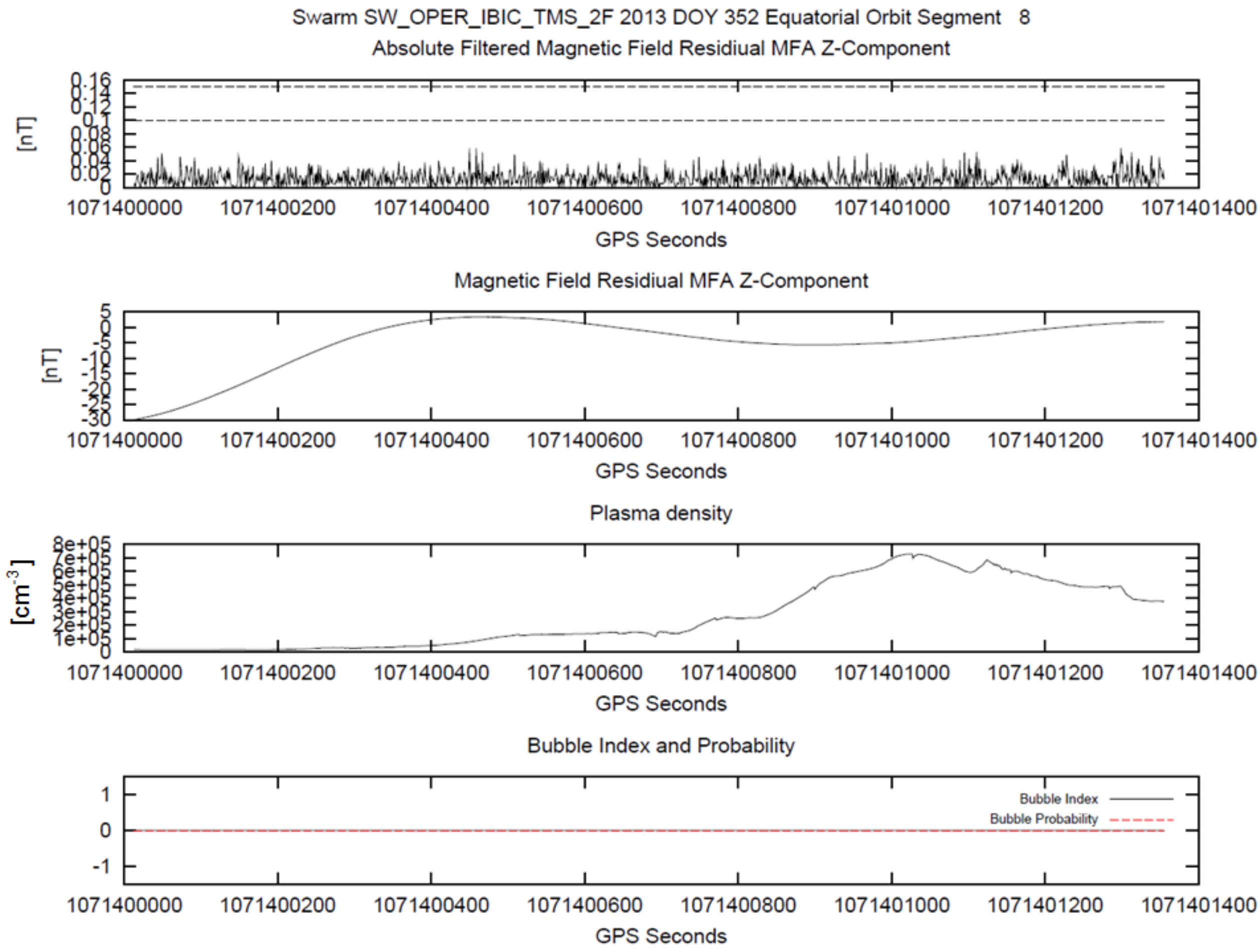

Figure 3: An example of Swarm L2-IBI data (Bubble Index=0; Quiet).

8 Statistical Distribution of Equatorial Plasma Bubbles

Figure 4 presents the statistical distribution (December 2013∼mid-August 2014) of plasma bubbles. The three panels correspond to the equinox, June solstice, and December solstice, respectively. Each solstice season is defined as 131 days around the solstice days, considering the local time precession of the Swarm satellites ($\sim$ 12 hours per 131 days). Similarly, the combined equinox is defined as the sum of $\pm$65 days around March and September equinoxes. The color represents bubble occurrence rate per bin, which is defined as the ratio between the number of data points affected by plasma bubbles (Bubble Index=1) and the total number of analyzable data points (Bubble Index$\neq -1$). Note that a 3-by-3 pixel median filter has been applied to Figure 4 and that data from all the three Swarm satellites (Alpha, Bravo, and Charlie) are included in Figure 4.

During June solstice (middle panel) the occurrence rate is high above Africa and the Pacific Ocean. During December solstice (bottom panel) global maximum of bubble occurrence rate exists near Brazil. The statistical bubble distribution during solstices (bottom two panels) is in general agreement with previous studies, such as RD2 and RD3. During equinox (top panel) the bubble occurrence rate is generally low while previous studies such as RD2 demonstrated that bubble occurrence rate is reasonably high irrespective of longitudes. This apparent discrepancy is because Swarm data for September equinox is not available yet, as of August 2014. As a result, the equinox plot in Figure 4 only consists of Swarm data around March 2014. During March 2014 the Swarm satellites were in the post-midnight local time, where bubble occurrence rate is very low and not representative of the whole bubble population: see RD2.

Note that an event detection threshold (the upper dashed line in Figures 1-3) of 0.15 nT was used for Figure 4. This value is lower than the values used by RD2 (0.25 nT) and by RD3 (0.2 nT). In order to check the dependence of the bubble climatology on the event detection threshold, we have run the IBI processor with two more values of event detection threshold: 0.2 nT for Figure 5 and 0.1 nT for Figure 6. The bubble climatology shown in Figures 4-6 is morphologically consistent with one another: (1) bubble hot spots in December solstice are around Brazil, (2) bubble hot spots in June solstice are around Africa and the Pacific Ocean, and (3) bubble encounter of Swarm satellites around March 2014 was generally rarer than during the other seasons.

Nevertheless, the optimal threshold is recommended to be 0.15 nT because L2-IBI with the threshold of 0.10 nT (Figure 6) found a considerable amount of bubbles where previous studies did not expect bubbles (e.g., near the mainland U.S. in the middle panel of Figure 6).

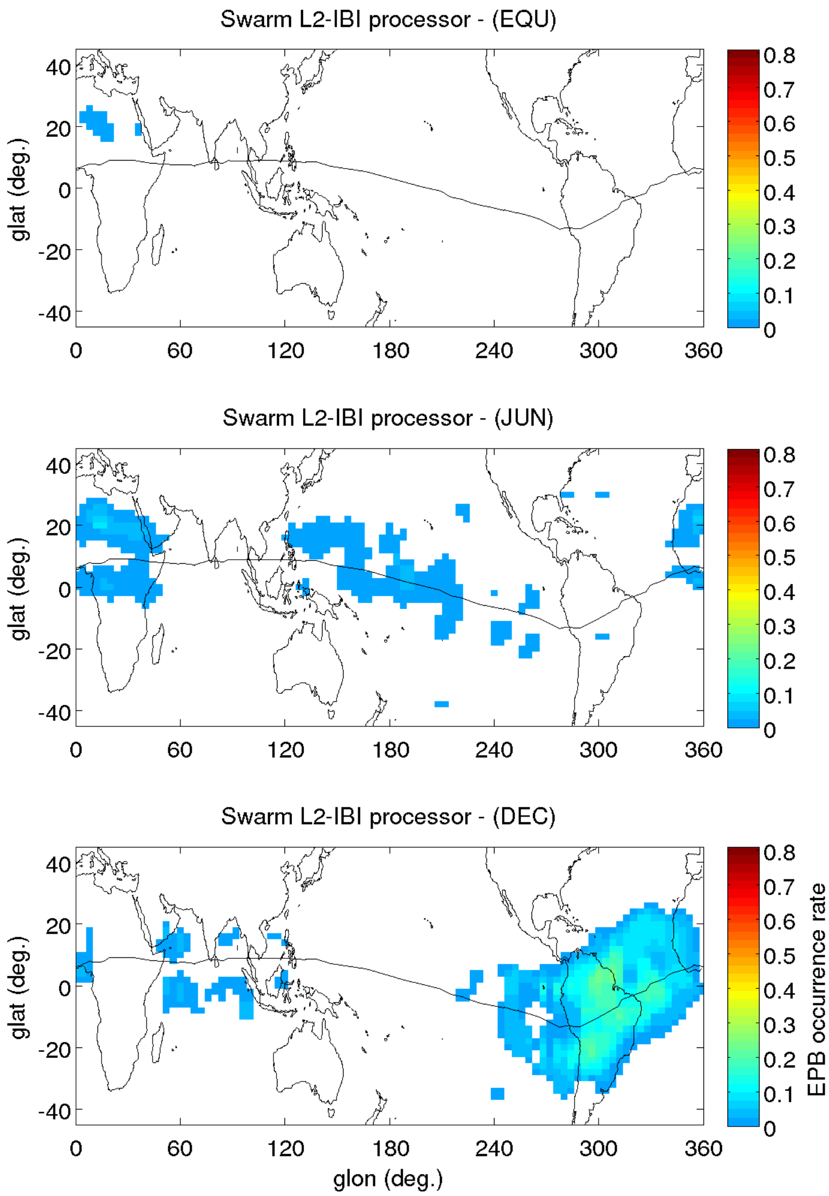

Figure 4: Statistical distribution of plasma bubbles (event detection threshold = 0.15 nT).

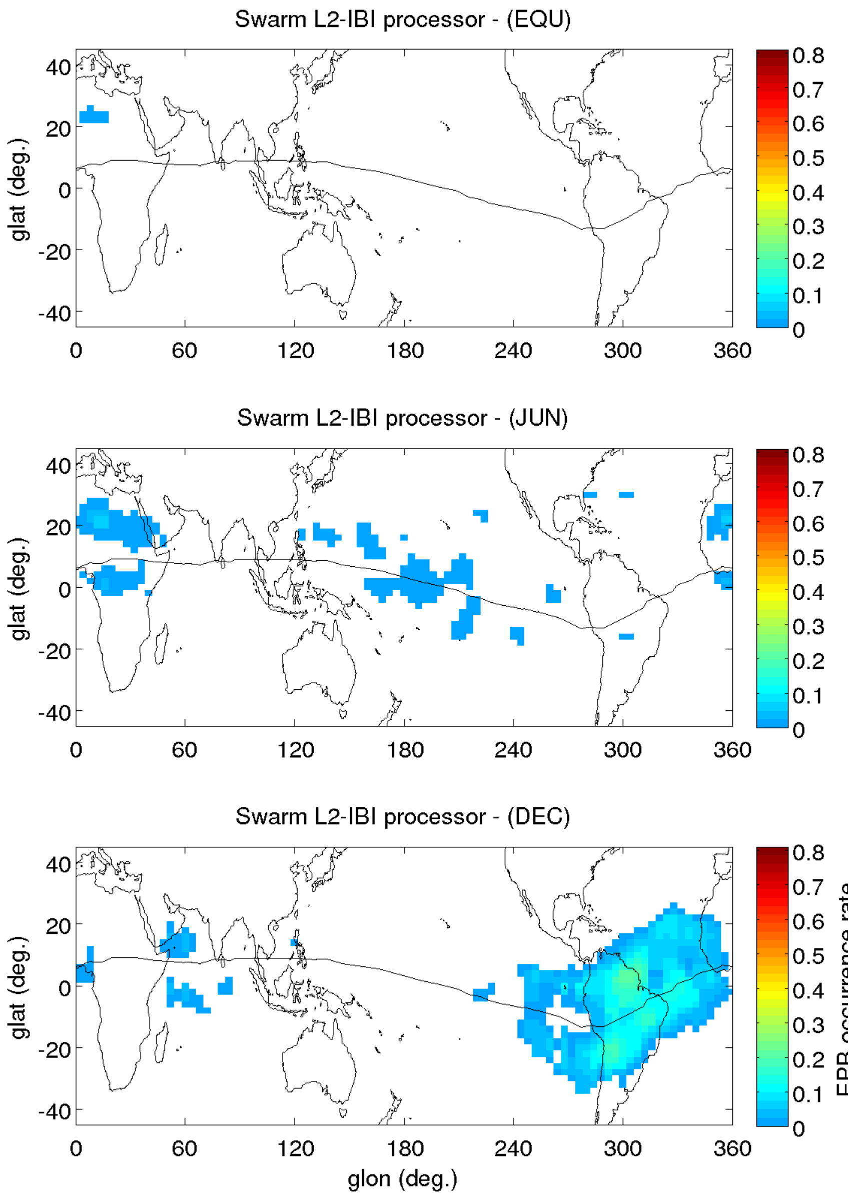

Figure 5: Statistical distribution of plasma bubbles (event detection threshold = 0.2 nT).

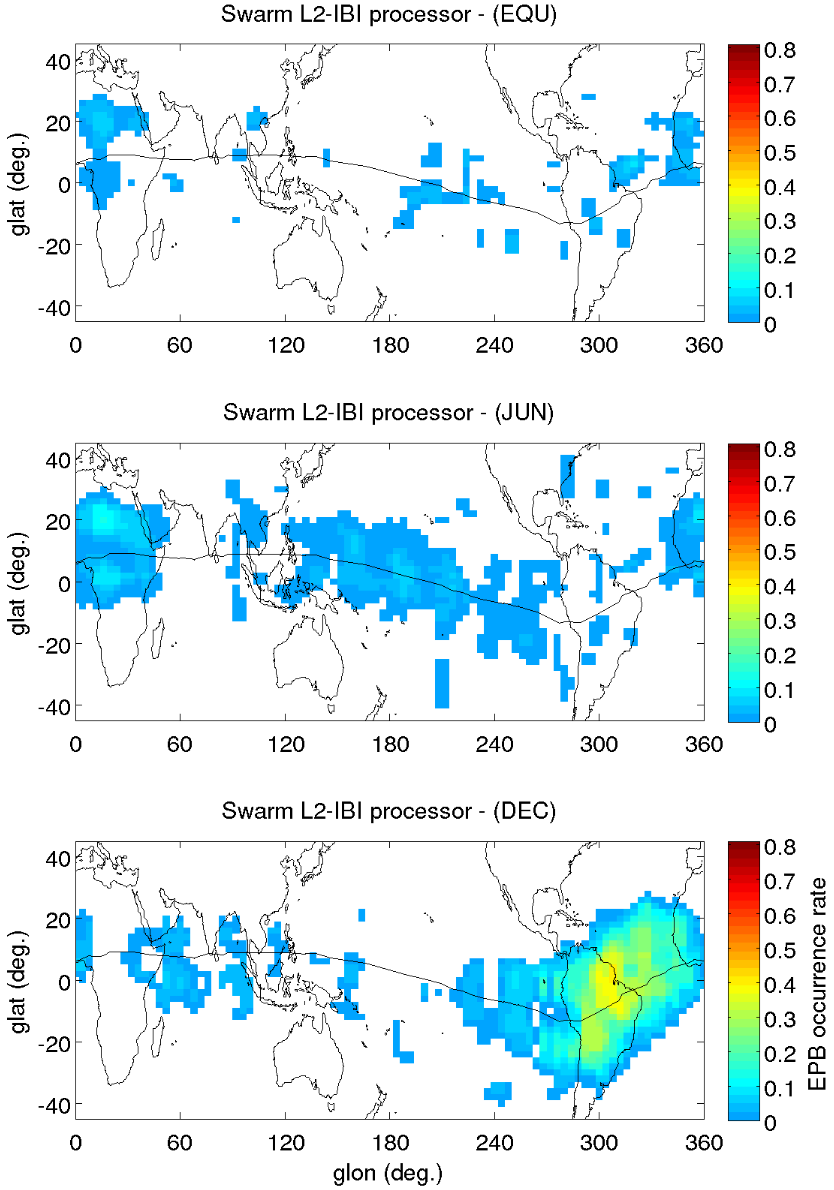

Figure 6: Statistical distribution of plasma bubbles (event detection threshold = 0.1 nT).

9 Conclusions

The results obtained confirm the scientific validity of the L2-IBI data (IBIATMS_2F, IBIBTMS_2F or IBICTMS_2F). The event detection threshold of 0.15 nT is recommended.